Current Microbiology (2024) 81:102
https://doi.org/10.1007/s00284-024-03615-x

Genome-Based Reclassification of *Anoxybacillus geothermalis* Filippidou et al. 2016 as a Later Heterotypic Synonym of *Anoxybacillus rupiensis* Derekova et al. 2007

Kadriye Inan Bektas[1] · Aleyna Nalcaoglu[1] · Halil İbrahim Guler[1] · Sabriye Canakci[2] · Ali Osman Belduz[2]

Received: 26 July 2023 / Accepted: 10 January 2024 / Published online: 20 February 2024

Abstract

In this study, our aim was to elucidate the relationship between *Anoxybacillus rupiensis* DSM 17127^T and *Anoxybacillus geothermalis* GSsed3^T through whole-genome phylogenetic analysis. The obtained 16S rRNA gene sequence from the genome of *A. rupiensis* DSM 17127^T exhibited a 99.8% similarity with *A. geothermalis* GSsed3^T. In the phylogenetic trees constructed using whole-genome sequences and 16S rRNA gene sequences, *A. rupiensis* DSM 17127^T and *A. geothermalis* GSsed3^T were observed to form a clade, indicating a close relationship between them. Moreover, the average amino acid identity, average nucleotide identity, and digital DNA–DNA hybridization values calculated between *A. rupiensis* DSM 17127^T and *A. geothermalis* GSsed3^T exceeded the threshold values typically used for species demarcation. Furthermore, the phylogenomic analysis based on the core genome of the strains in question provided additional support for the formation of a monophyletic clade by *A. rupiensis* DSM 17127^T and *A. geothermalis* GSsed3^T. Most phenotypic and chemotaxonomic features between both strains were almost identical except for a few exceptions. These findings suggest that both strains should be classified as belonging to the same species, and we propose that *A. geothermalis* GSsed3^T is a later heterotypic synonym of *A. rupiensis* DSM 17127^T.

Introduction

The genus *Anoxybacillus*, which belongs to the phylum *Firmicutes*, was initially proposed by Pikuta et al. in 2000 [1], with *Anoxybacillus pushchinoensis* as the type species. Its description was subsequently amended by Pikuta et al. in 2003 [2]. At the time of writing, there are 24 species within this genus with validly published names, along with three species that have not been validly published (http://www.bacterio.net). *Anoxybacillus* species are widely distributed and can be found in geothermally heated environments. The taxonomic classification of *Anoxybacillus* members has traditionally relied on 16S rRNA gene sequence analysis and DNA–DNA hybridization (DDH). However, it is known that the discriminatory power of 16S rRNA gene analysis is often limited when it comes to distinguishing closely related species, such as those within the *Anoxybacillus* genus. DDH is a time-consuming and labor-intensive method, and the establishment of a central database is impractical. Recently, phylogenetic approaches utilizing whole-genome sequence-based metrics, such as average nucleotide identity (ANI), digital DDH (dDDH), and average amino acid identity (AAI), have emerged as important tools for the classification of prokaryotic taxa. These methods have been employed in the reclassification of various bacterial taxa [3, 4].

Anoxybacillus rupiensis DSM 17127^T was isolated from different springs in the area of Rupi basin by Derekova et al. in 2007 [5] and its validation was documented in the International Journal of Systematic and Evolutionary Microbiology (Validation List No. 119) [6]. *Anoxybacillus geothermalis* GSsed3^T was isolated from deposits at the entrance filters of the geothermal research facility of Groß Schönebeck in northern Germany by Filippidou et al. in 2016 [7], as validly named species. In the original article, Filippidou et al. [7] proposed *A. geothermalis* GSsed3^T as a new species within the genus *Anoxybacillus*, primarily based on the DNA–DNA hybridization (DDH) value between *A. rupiensis* DSM

✉ Kadriye Inan Bektas
kadriyensis@gmail.com

[1] Department of Molecular Biology and Genetics, Faculty of Science, Karadeniz Technical University, 61080 Trabzon, Turkey

[2] Department of Biology, Faculty of Science, Karadeniz Technical University, 61080 Trabzon, Turkey

17127^T and *A. geothermalis* GSsed3^T and based on genomic average nucleotide identity (ANI) value and pairwise digital DNA–DNA hybridization (dDDH) values between *A. amylolyticus* MR3C^T and *A. geothermalis* GSsed3^T. Due to the unavailability of the genome sequence of *A. rupiensis* DSM 17127^T in any database, Filippidou et al. [7] were unable to determine the average nucleotide identity (ANI) value and pairwise digital DNA–DNA hybridization values between *A. rupiensis* DSM 17127^T and *A. geothermalis* GSsed3^T. During our genome-based analysis, we observed that *A. rupiensis* DSM 17127^T and *A. geothermalis* GSsed3^T shared similar features. As a result, we attempted to clarify the relationship between *A. rupiensis* DSM 17127^T and *A. geothermalis* GSsed3^T using genomics-based methods. The data presented in this study provide evidence that *A. geothermalis* GSsed3^T is a later heterotypic synonym of *A. rupiensis* DSM 17127^T.

Materials and Methods

A. rupiensis DSM 17127^T and *A. geothermalis* GSsed3^T were obtained from the German Collection of Microorganisms and Cell Cultures GmbH (DSMZ). Two type strains were cultivated on Nutrient Agar medium and incubated at a temperature of 55 °C for a duration of 24 h. In this study, the genome sequence of *A. rupiensis* DSM 17127^T was determined, while the genome sequence of *A. geothermalis* GSsed3^T (JYCG00000000) was downloaded from the GenBank database. For the complete genome sequencing, genomic DNA was isolated from *A. geothermalis* GSsed3^T culture using the QIAamp DNA Mini Kit according to the manufacturer's instructions. The whole-genome sequencing of *A. geothermalis* GSsed3^T was performed using 2 × 250 bp paired-end reads on an Illumina HiSeq 2500 platform by MicrobesNG (University of Birmingham, United Kingdom). The reads were assembled using the complete SPAdes assembly strategy on the PATRIC web server (https://patricbrc.org/) [8]. Genome annotation was performed using Rapid Annotations using Subsystems Technology (RAST) server [9]. The draft genome sequences obtained in this study have been submitted to the National Center for Biotechnology Information (NCBI) database and can be accessed under the accession number JAQOTG010000000.

The pairwise alignment feature implemented on the EZBioCloud server (https://www.ezbiocloud.net/tools/pairAlign) was used to compare the 16S rRNA gene sequence identity between *A. rupiensis* DSM 17127^T and *A. geothermalis* GSsed3^T. The 16S rRNA gene sequences of closely related type strains were obtained from the EzBioCloud server at https://www.ezbiocloud.net/ [10] and subsequently edited using the BioEdit software [11]. The ClustalW program [12] was employed for multiple sequence alignment of the 16S rRNA gene sequences. The Kimura's two-parameter model [13] was employed to calculate the evolutionary distances. The phylogenetic trees were constructed using Mega-X software, employing the neighbor-joining method [14], maximum-parsimony method (Kluge and Farris, 1969), and maximum-likelihood method [15]. The bootstrap values were determined based on 1000 replications to assess the robustness of the tree topologies.

The phylogenetic analysis of *A. rupiensis* DSM 17127^T and *A. geothermalis* GSsed3^T was conducted using the type strain genomes server pipeline (TYGS) developed by Meier-Kolthoff and Göker [16]. The digital DNA–DNA hybridization (dDDH) value between the draft genome sequences of *A. rupiensis* DSM 17127^T and *A. geothermalis* GSsed3^T was calculated using Formula 2 of the online Genome-to-Genome Distance Calculator (GGDC) tool provided at http://ggdc.dsmz.de/distcalc2.php, as proposed by Meier-Kolthoff et al. [17]. To assess the genetic relationship between *A. rupiensis* DSM 17127^T and *A. geothermalis* GSsed3^T, average nucleotide identity (ANI) values were determined using the orthoANIu algorithm and an online ANI calculator available at www.ezbiocloud.net/tools/ani, as described by Lee et al. [18] and Yoon et al. [19]. A phylogenetic tree based on whole-genome sequences was constructed using the TYGS web server developed by Meier-Kolthoff and Göker [16]. The amino acid identity (AAI) value was calculated using the CompareM software (https://github.com/dparks1134/CompareM).

For the phylogenetic and pangenome analyses, the genomes of *A. rupiensis* DSM 17127^T and *A. geothermalis* GSsed3^T and all other *Anoxybacillus* species registered in RefSeq were re-annotated using Prokka 1.14.5 with default settings to ensure consistent annotation [20]. Phylogenetic trees were constructed using the 'insert genome into species tree app' version 2.2.0, which utilizes the FastTree 2 algorithm developed by Price et al. [21]. The pangenome was constructed using the 'build pangenome with OrthoMCL app' version 2.0, available on the KBase platform (https://www.kbase.us/), as described by Arkin et al. [22]. Pangenome-based phylogenomic analysis was performed using the 'phylogenetic pangenome accumulation app' version 1.4.0 developed by Li et al. [23] and Arkin et al. [22].

The assessment of *A. rupiensis* DSM 17127^T and *A. geothermalis* GSsed3^T's biochemical characteristics was conducted using the API 20E, API 50CH strips, and the Vitek2 Bacilli Identification Card (BCL) microtest systems from bioMérieux, adhering to the instructions provided by the manufacturer. The polar lipids of strain *A. salavatliensis* DSM 22626^T and *A. gonensis* G2^T were extracted from 100-mg freeze-dried cells using two-dimensional thin-layer chromatography (TLC) according to the method of Tindall [24, 25]. Two-dimensional TLC on silica gel facilitated the separation of polar lipids. The initial phase involved the

use of chloroform:methanol:water (65:25:4, v/v), while the subsequent phase utilized chloroform:methanol:acetic acid:water (80:12:15:4, v/v). For the detection process, 5% ethanolic molybdophosphoric acid was employed for total lipids, molybdenum blue for phospholipids, ninhydrin for aminolipids, and α-naphthol for glycolipids, as per the methodology outlined by Tindall et al. [26]. Reference standards included diphosphatidylglycerol (DPG), phosphatidic acid (PA), phosphatidylglycerol (PG), phosphatidylethanolamine (PE), phosphatidylcholine (PC), phosphatidylserine (PS), and phosphatidylinositol (PI). Extracting and purifying isoprenoid quinones from freeze-dried cells involved adhering to Collins' procedure [27] and subjected the samples to analysis using high-performance liquid chromatography (HPLC).

Results and Discussion

Whole-genome sequencing has greatly contributed to resolving the taxonomic inconsistencies within prokaryotic taxa, leading to the reclassification of several bacterial species [28]. In this study, we conducted a comprehensive reassessment of the taxonomic relationship between *A. rupiensis* DSM 17127^T and *A. geothermalis* GSsed3^T by employing whole-genome phylogenetic analysis. *A. geothermalis* GSsed3^T was isolated from deposits at the entrance filters of the geothermal research facility of Groß Schönebeck in northern Germany, while *A. rupiensis* DSM 17127^T was isolated from different springs in the area of Rupi basin.

In their original study, Filippidou et al. [7] reported that *A. geothermalis* GSsed3^T exhibited a 16S rRNA gene sequence similarity of 99.8% with *A. rupiensis* DSM 17127^T. However, despite this high similarity, they reported that the DNA–DNA hybridization value between *A. rupiensis* DSM 17127^T and *A. geothermalis* GSsed3^T was determined to be 16%, which is below the species delineation threshold (70%) as defined by Wayne et al. [29]. In this study, we conducted a comprehensive analysis to assess the phylogenetic relationship between *A. rupiensis* DSM 17127^T and *A. geothermalis* GSsed3^T, focusing on various genomic parameters. The pairwise nucleotide sequence alignment of their 16S rRNA gene sequences revealed a high similarity of 99.8%, with three nucleotide mismatches. Furthermore, phylogenetic tree reconstructions based on the 16S rRNA gene sequences consistently clustered *A. rupiensis* DSM 17127^T and *A. geothermalis* GSsed3^T together in the neighbor-joining algorithm, showing robust clustering with a high bootstrap resampling value of 96% (Fig. 1). Similar results were obtained when employing the maximum-likelihood and maximum-parsimony algorithms (Figs. S1, S2), further supporting their close phylogenetic relationship.

In the phylogenomic tree (Fig. 2), *A. rupiensis* DSM 17127^T and *A. geothermalis* GSsed3^T formed a distinct and well-supported branch separate from other type strains within the same genus, with a high bootstrap resampling value of 100%. The average nucleotide identity (ANI) value between *A. rupiensis* DSM 17127^T and *A. geothermalis* GSsed3^T was determined to be 98.60%, surpassing the suggested threshold value (95–96%) for species demarcation [30]. This finding confirms their high phylogenetic relatedness at the genomic level. Moreover, the average amino acid identity (AAI) value between *A. rupiensis* DSM 17127^T and *A. geothermalis* GSsed3^T was calculated as 98.50%, significantly exceeding the recommended cut-off for species delineation (AAI > 95%) [31], further supporting their classification within the same species. Furthermore, digital DNA–DNA hybridization (dDDH) analyses yielded a dDDH value of 85.6% between *A. rupiensis* DSM 17127^T and *A. geothermalis* GSsed3^T, surpassing the established cut-off (70%) for assigning bacterial strains to the same species [29]. These results reinforce the notion that *A. geothermalis* GSsed3^T and *A. rupiensis* DSM 17127^T should be considered members of the same species. Table 1 presents the AAI, ANI, and dDDH values calculated between *A. rupiensis* DSM 17127^T, *A. geothermalis* GSsed3^T, and other closely related type strains.

The pangenomic analysis of *Anoxybacillus* species, including *A. rupiensis* DSM 17127^T and *A. geothermalis* GSsed3^T, resulted in the identification of 9726 orthologous clusters that constituted the pangenome. The numbers of core genes, strain-specific genes (singleton), and accessory genes (partial) were 128, 5062, and 4536, respectively. According to the pangenome-based phylogenomic analysis, *A. rupiensis* DSM 17127^T and *A. geothermalis* GSsed3^T formed a monophyletic clade and shared 2421 core genes, indicating their close evolutionary relationship (Fig. 3).

Furthermore, the validation of this conclusion has been established through a comparison of phenotypic and chemotaxonomic characteristics between *A. rupiensis* DSM 17127^T and *A. geothermalis* GSsed3^T. In the API 20E, API 50CH, and Vitek2 BCL system, *A. rupiensis* DSM 17127^T and *A. geothermalis* GSsed3^T exhibited similar biochemical features with minor exceptions (Table 2). As an illustration, acid production from D-galactose, sucrose, and arginine dihydrolase were negative for *A. rupiensis* DSM 17127^T, whereas *A. geothermalis* GSsed3^T showed positive results. On the other hand, urease, ornithine decarboxylase, tryptophanase, and acid production from D-trehalose and D-mannose were positive for *A. rupiensis* DSM 17127^T, whereas *A. geothermalis* GSsed3^T yielded negative results. Both species exhibited positive results for lysine decarboxylase, tyrosine arylamidase, citrate utilization, catalase, phenylalanine arylamidase, Ala-Phe-Pro-Arylamidase, α-glucosidase acid

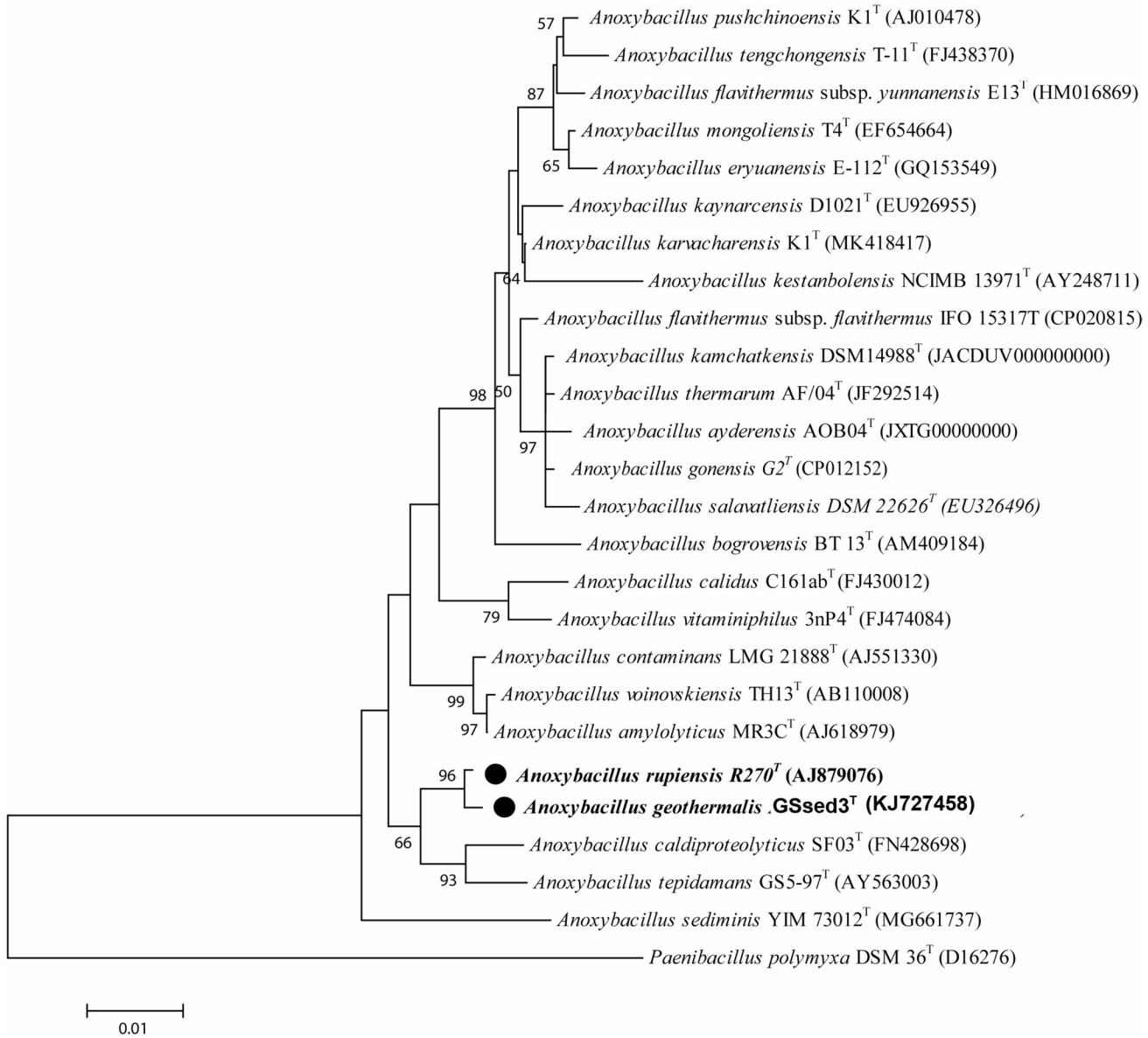

Fig. 1 Neighbor-joining (NJ) tree constructed based on 16S rRNA gene sequences available from the GenBank database. Bootstrap values (expressed as percentages of 1000 replications) greater than 50% are shown at branch points. Bar, 0.01 represents substitutions per nucleotide position. *Paenibacillus polymyxa* DSM 36^T was used as the outgroup

production from D-xylose, D-mannitol, D-glucose, D-fructose, D-ribose, D-maltose, glycerol, esculin ferric citrate, D-saccharose, and starch. Also, *A. rupiensis* DSM 17127^T and *A. geothermalis* GSsed3^T exhibited negative results for nitrate reduction, leucine-arylamidase, tryptophan deaminase, glycine arylamidase, gelatin hydrolysis, Voges–Proskauer, β-galactosidase, polymyxin B resistance, L-proline arylamidase, β-N-acetyl-glucosaminidase, hydrogen sulfide production, L-lysine arylamidase, alanine arylamidase, pyruvate, β-xylosidase, L-aspartate arylamidase, L-pyrrolydonyl arylamidase, phosphoryl choline, cyclodextrine, methyl-D-xyloside, α-mannosidase, N-acetyl-glucosamine, kanamycin resistance, β-mannosidase, methyl-a-D-glucopyranoside, salicin, D-cellobiose, D-trehalose, inulin, D-melezitose, glycogen, D-turanose, growth in 6.5% NaCI, oleandomycin resistance, acid production from L-arabinose, D-sorbitol, D-melibiose, L-xylose, D-raffinose, D-tagatose, D-arabitol, arbutin, inositol, L-rhamnose, putrescine, erythritol, D-arabinose, methyl-D-xylopyranoside, L-sorbose, dulcitol, amygdalin, D-lactose, xylitol, gentiobiose, D-lyxose, D-fucose, L-fucose, L-arabitol, potassium gluconate, potassium 2-ketogluconate, and potassium 5-ketogluconate. The total count of phenotypic tests conducted utilizing the API 20E, API 50CH, and Vitek2 BCL system amounted to 91.

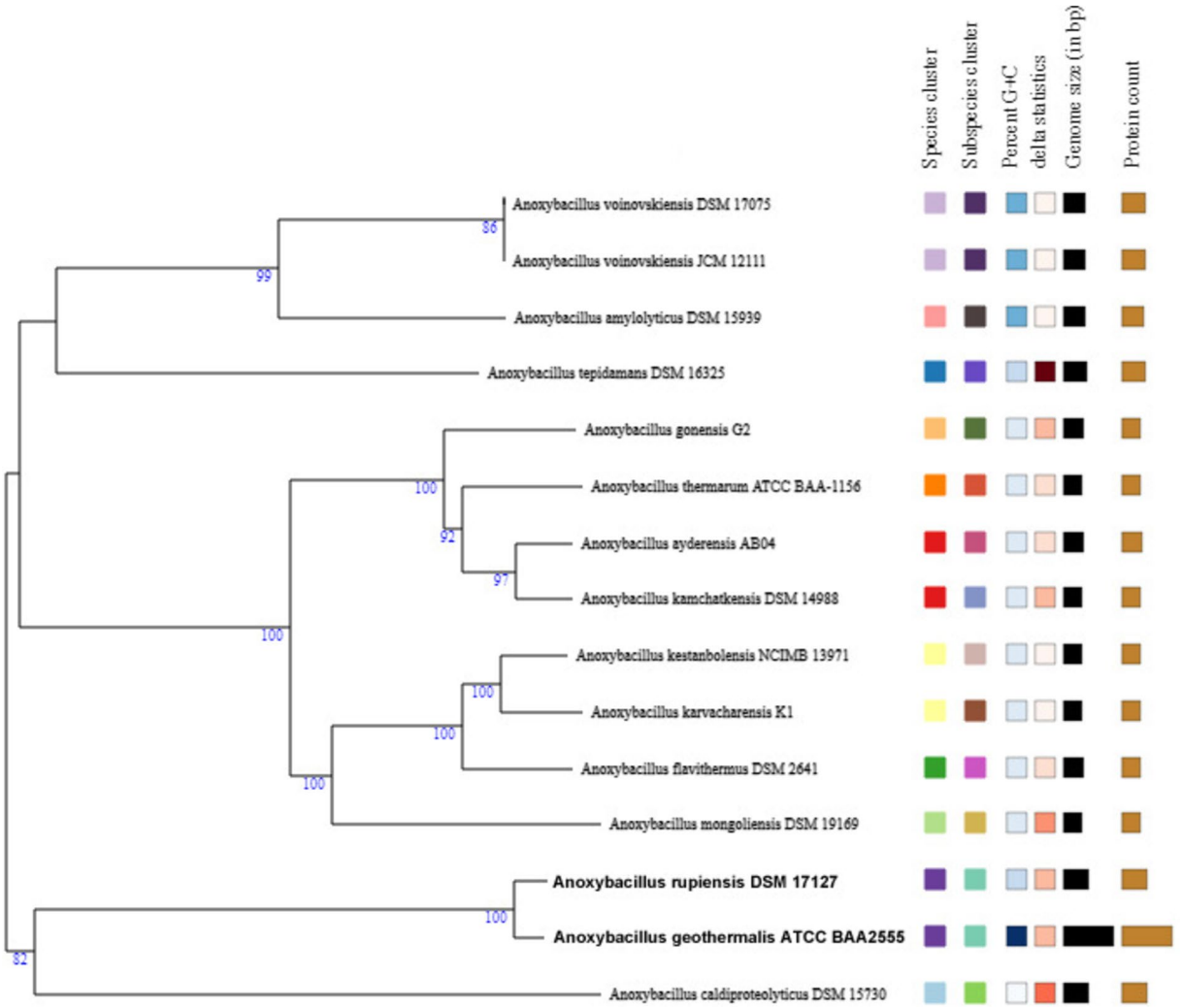

Fig. 2 Phylogenetic tree based on whole-genome sequences of *A. rupiensis* DSM 17127^T and *A. geothermalis* GSsed3^T and related reference strains. The tree was inferred with FastME 2.1.6.1 [33] from genome blast distance phylogeny (GBDP) distances calculated from genome sequences using the TYGS server (https://tygs.dsmz.de) [16]. The branch lengths are scaled in terms of GBDP distance formula d5. The numbers at branches are GBDP pseudo-bootstrap support values ≥ 64% from 100 replications with an average branch support of 97.7%. The tree was rooted at the midpoint [34] (Color figure online)

Table 1 AAI, ANI and dDDH values between *A. rupiensis* DSM 17127^T, *A. geothermalis* GSsed3^T, and closely related type strains

	A. rupiensis DSM 17127^T			*A. geothermalis* GSsed3^T		
	AAI	ANI	dDDH	AAI	ANI	dDDH
A. rupiensis DSM 17127^T (JAQOTG010000000)	–	–	–	98.5	98.60	85.60
A. geothermalis GSsed3^T (JYCG00000000)	98.5	98.60	85.60	–	–	–
A. tepidimanas DSM 16325^T (JACHEP000000000.1)	82.5	79.11	22.00	81.8	78.95	21.90
A. amylolyticus DSM 15939^T (NZ_CP015438)	80.2	77.56	20.70	79.9	77.62	20.80
A. voinovskiensis JCM 12111^T (BMNP00000000.1)	80.4	77.88	20.70	79.6	77.91	20.90
A. caldiproteolyticus DSM 15730^T (NZ_CP064060)	79.8	77.53	20.50	79.6	77.65	20.40

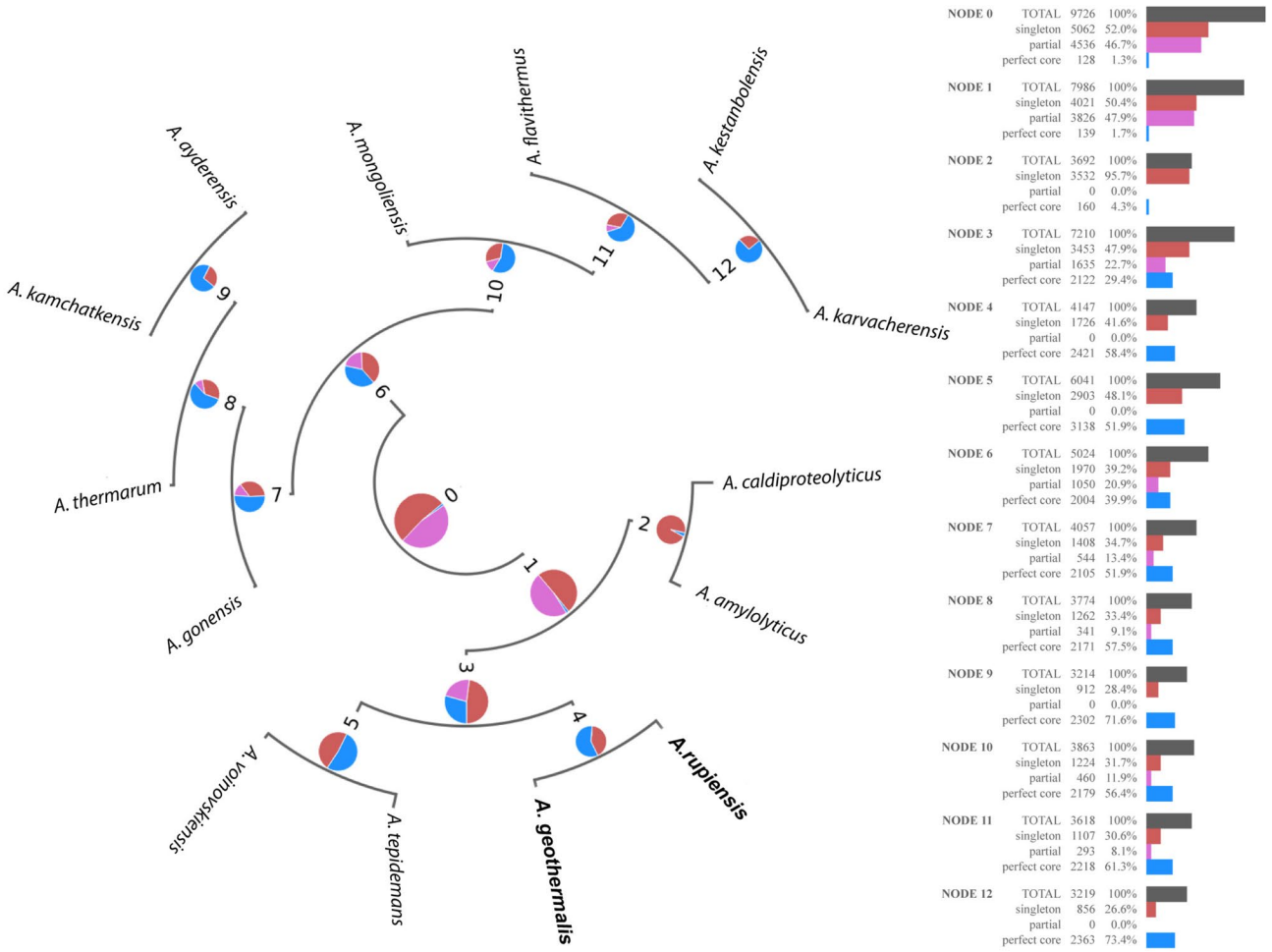

Fig. 3 Pangenome-based phylogenomic analysis of *Anoxybacillus* species. Orthologous gene sets within a pangenome are partitioned into three categories: core (blue), singleton (red), and partial pangenome (pink). Pangenome-based phylogenomic analysis was created by the OrthoMCL and phylogenetic pangenome accumulation (v1.4.0) app (Color figure online)

It was determined that there was a difference between *A. rupiensis* DSM 17127^T and *A. geothermalis* GSsed3^T in only 8 tests and the difference value was 9%.

In the original article, Derekova et al. [5] were not determined the polar lipids of *A. rupiensis* DSM 17127^T. In the present study, the polar lipids found in *A. rupiensis* DSM 17127^T were diphosphatidylglycerol (DPG), phosphatidylglycerol (PG), phosphatidylethanolamine (PE), unidentified amino phospholipid (APL), unidentified phospholipid-1 (PL1), unidentified phospholipid-2 (PL2), unidentified lipid-1 (L1), unidentified lipid-2 (L2), and unidentified lipid-3 (L3), whereas *A. geothermalis* GSsed3^T consisted of DPG, PG, PE, APL, PL1, L1, and L3. Polar lipid composition showed very similar profile between two species (Fig. 4). The respiratory quinone of *A. rupiensis* DSM 17127^T and *A. geothermalis* GSsed3^T was menaquinone MK-7. Most of the chemotaxonomic and phenotypic features between *A. rupiensis* DSM 17127^T and *A. geothermalis* GSsed3^T were almost identical except for a few exceptions as is shown in Table 2 and Fig. 4. The disagreement for phenotypic and chemotaxonomic was probably due to their different ecological niches.

Collectively, the findings of this study indicate that *A. rupiensis* DSM 17127^T and *A. geothermalis* GSsed3^T should be regarded as the same species. Therefore, based on the phylogenetic analysis using whole-genome sequences and following rule 42 of the Bacteriological Code [32], we propose that *A. geothermalis* GSsed3^T, originally described by Filippidou et al. in 2016 [7], be reclassified as a later heterotypic synonym of *A. rupiensis* DSM 17127^T, as initially described by Derekova et al. in 2007. The type strain for *A. rupiensis* is DSM 17127^T (= R270^T = NBIMCC 8387^T), and GSsed3 (= CCOS808 = ATCC BAA2555) represents an additional strain of *A. rupiensis*.

Table 2 The biochemical characteristics of *A. geothermalis* GSsed3^T and *A. rupiensis* DSM 17127^T

	A. geothermalis GSsed3^T	*A. rupiensis* DSM 17127^T
Arginine dihydrolase	+	−
Urease	−	+
Ornithine decarboxylase	−	+
Tryptophanase	−	+
Tyrosine arylamidase	+	+
Lysine decarboxylase	+	+
Polymycin B resistance	−	−
β-galactosidase	−	−
L-proline arylamidase	−	−
β-N-acetyl-glucosaminidase	−	−
Hydrogen sulfide production	−	−
Gelatin hydrolysis	−	−
Leucine-arylamidase	−	−
Tryptophan deaminase	−	−
Glycine arylamidase	−	−
Acid production from:		
Sucrose	+	−
D-galactose	+	−
D-trehalose	−	+
D-mannose	−	+
D-xylose	+	+
L-arabinose	+	+
D-glucose	+	+
D-maltose	+	+
D-fructose	+	+
D-mannitol	+	+
D-ribose	+	+
L-arabinose	−	−
D-sorbitol	−	−
D-melibiose	−	−
L-xylose	−	−
D-raffinose	−	−
D-tagatose	−	−
D-arabitol	−	−
Arbutin	−	−

+ positive, − negative

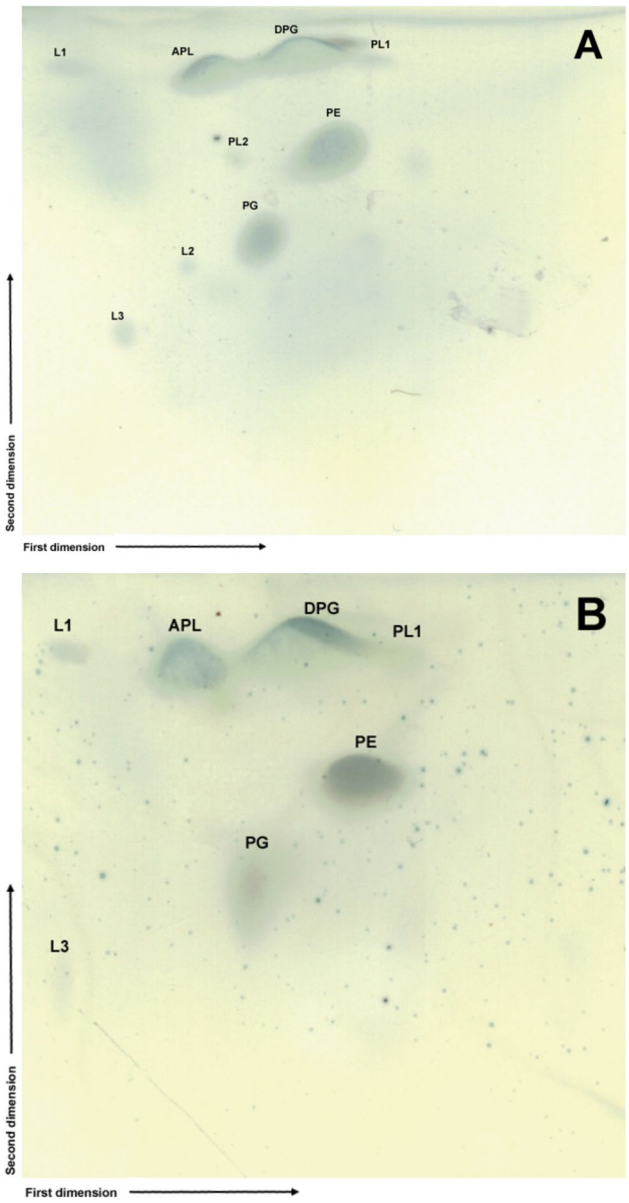

Fig. 4 Two-dimensional thin-layer chromatogram of polar lipids of **A** *A. rupiensis* DSM 17127^T and **B** *A. geothermalis* GSsed3^T. *DPG* diphosphatidylglycerol, *PG* phosphatidylglycerol, *PE* phosphatidylethanolamine, *APL* unidentified aminophospolipid, *PL* unidentified phospholipid, *L* unidentified lipid (Color figure online)

Emended Species Description of *Anoxybacillus rupiensis* Derekova et al. 2007

Anoxybacillus rupiensis (N.L. masc. adj. rupiensis, originating from Rupi Basin, referring to the place of isolation of the type strain).

The description is the same as given by Derekova et al. (2007) with the following modification.

The respiratory quinone is menaquinone MK-7. Major polar lipids include diphosphatidylglycerol (DPG), phosphatidylglycerol (PG), phosphatidylethanolamine (PE), unidentified amino phospholipid (APL), unidentified phospholipid-1 (PL1), unidentified phospholipid-2 (PL2), unidentified lipid-1 (L1), unidentified lipid-2 (L2), and unidentified lipid-3 (L3). In API 50CH, API 20E, and Vitek2 BCL system, the following activities were positive for lysine decarboxylase, tyrosine arylamidase, citrate utilization, catalase, phenylalanine arylamidase, Ala-Phe-Pro-Arylamidase, α-glucosidase, urease, ornithine decarboxylase, tryptophanase and acid production from D-trehalose,

D-mannose, D-xylose, D-mannitol, D-glucose, D-fructose, D-ribose, D-maltose, glycerol, esculin ferric citrate, D-saccharose, and starch. Negative for nitrate reduction, leucine arylamidase, tryptophan deaminase, glycine arylamidase, gelatin hydrolysis, Voges–Proskauer, β-galactosidase, polymyxin B resistance, L-proline arylamidase, β-N-acetyl-glucosaminidase, hydrogen sulfide production, L-lysine arylamidase, alanine arylamidase, pyruvate, β-xylosidase, L-aspartate arylamidase, L-pyrrolydonyl arylamidase, phosphoryl choline, cyclodextrine, methyl-D-xyloside, α-mannosidase, N-acetyl-glucosamine, kanamycin resistance, β-mannosidase, methyl-a-D-glucopyranoside, salicin, D-cellobiose, D-trehalose, inulin, D-melezitose, glycogen, D-turanose, growth in 6.5% NaCI, oleandomycin resistance, acid production from L-arabinose, D-sorbitol, D-melibiose, L-xylose, D-raffinose, D-tagatose, D-arabitol, arbutin, inositol, L-rhamnose, putrescine, erythritol, D-arabinose, methyl-D-xylopyranoside, L-sorbose, dulcitol, amygdalin, D-lactose, xylitol, gentiobiose, D-lyxose, D-fucose, L-fucose, L-arabitol, potassium gluconate, potassium 2-ketogluconate, and potassium 5-ketogluconate. The DNA G + C content of the type strain 17127^T (= R270^T = NBIMCC 8387^T) is 42.27 mol% (genome-based).

Supplementary Information The online version contains supplementary material available at https://doi.org/10.1007/s00284-024-03615-x.

Author Contributions KIB designed the study. KIB, AOB, and SC performed genome analysis. KIB, HIB, and AN analyzed the data and wrote the manuscript. All authors read and approved the final manuscript.

Funding This study was supported by Karadeniz Technical University (KTU BAP FAT-2019-7822).

Declarations

Conflict of interest The authors declare that there is no conflict of interest.

Ethical Approval This article does not contain any studies with human participants or animals performed by any of the authors.

References

1. Pikuta E, Lysenko A, Chuvilskaya N, Mendrock U et al (2000) *Anoxybacillus pushchinensis* gen. nov., sp. nov., a novel anaerobic, alkaliphilic, moderately thermophilic bacterium from manure, and description of *Anoxybacillus flavithermus* comb. nov. Int J Syst Evol Microbiol 50:2109–2117. https://doi.org/10.1099/00207713-50-6-2109
2. Pikuta E, Cleland D, Tang J (2003) Aerobic growth of *Anoxybacillus pushchinoensis* K1T: emended descriptions of *A. pushchinoensis* and the genus Anoxybacillus. Int J Syst Evol Microbiol 53:1561–1562. https://doi.org/10.1099/ijs.0.02643-0
3. Liu GH, Rao MPN, Dong ZY, Wang JP, Che JM, Chen QQ, Sengonca C, Liu B, Li WJ (2019) Genome-based reclassifcation of *Bacillus plakortidis* Borchert et al. 2007 and *Bacillus lehensis* Ghosh et al. 2007 as a later heterotypic synonym of *Bacillus oshimensis* Yumoto et al. 2005; *Bacillus rhizosphaerae* Madhaiyan et al. 2011 as a later heterotypic synonym of *Bacillus clausii* Nielsen et al. 1995. Anton Leeuw 112:1725–1730. https://doi.org/10.1007/s10482-019-01299-z
4. Rao MPN, Xiao M, Liu D, Tang R, Liu G, Li W (2022) Genome-based reclassifcation of *Evansella polygoni* as a later heterotypic synonym of *Evansella clarkii* and transfer of *Bacillus shivajii* and *Bacillus tamaricis* to the genus Evansella as *Evansella shivajii* comb. nov. and *Evansella tamaricis* comb. nov. Arch Microbiol 204:47. https://doi.org/10.1007/s00203-021-02720-w
5. Derekova A, Sjøholm C, Mandeva R, Kambourova M (2007) *Anoxybacillus rupiensis* sp. nov., a novel thermophilic bacterium isolated from Rupi basin (Bulgaria). Extremophiles 11:577–583. https://doi.org/10.1007/s00792-007-0071-4
6. Euzeby JP (2008) Validation list no. 119. List of new names and new combinations previously effectively, but not validly, published. Int J Syst Evol Microbiol 58:1–2
7. Filippidou S, Jaussi M, Junier T et al (2016) *Anoxybacillus geothermalis* sp. nov., a facultatively anaerobic, endospore-forming bacterium isolated from mineral deposits in a geothermal station. Int J Syst Evol Microbiol 66:2944–2951. https://doi.org/10.1099/ijsem.0.001125
8. Wattam AR, Davis JJ, Assaf R et al (2017) Improvements to PATRIC, the all-bacterial bioinformatics database and analysis resource center. Nucleic Acid Res 45:D535–D542. https://doi.org/10.1093/nar/gkw1017
9. Aziz RK, Bartels D, Best AAB et al (2008) The RAST Server: rapid annotations using subsystems technology. BMC Genomics 9:75. https://doi.org/10.1186/1471-2164-9-75
10. Yoon SH, Ha SM, Kwon S, Lim J, Kim Y, Seo H, Chun J (2017) Introducing EzBioCloud: a taxonomically united database of 16S rRNA and whole genome assemblies. Int J Syst Evol Microbiol 67:1613–1617. https://doi.org/10.1099/ijsem.0.001755
11. Hall TA (1999) BioEdit: a user-friendly biological sequence alignment editor and analysis program for Windows 95/98/NT. Nucleic Acids Symp Ser 41:95–98. https://doi.org/10.14601/Phytopathol_Mediterr-14998u1.29
12. Thompson JD, Higgins DG, Gibson TJ (1994) CLUSTAL W: improving the sensitivity of progressive multiple sequence alignment through sequence weighting, position-specific gap penalties and weight matrix choice. Nucleic Acids Res 22:4673–4680. https://doi.org/10.1093/nar/22.22.4673
13. Kimura M (1980) A simple method for estimating evolutionary rates of base substitutions through comparative studies of nucleotide sequences. J Mol Evol 16:111–120. https://doi.org/10.1007/bf01731581
14. Saitou N, Nei M (1987) The neighbor-joining method: a new method for reconstructing phylogenetic trees. Mol Biol Evol 4:406–425. https://doi.org/10.1093/oxfordjournals.molbev.a040454
15. Felsenstein J (1981) Evolutionary trees from DNA sequences: a maximum likelihood approach. J Mol Evol 17:368–376. https://doi.org/10.1007/bf01734359
16. Meier-Kolthoff JP, Göker M (2019) TYGS is an automated high-throughput platform for state-of-the-art genome-based taxonomy. Nat Commun 10(1):2182. https://doi.org/10.1038/s41467-019-10210-3
17. Meier-Kolthoff JP, Auch AF, Klenk HP, Göker M (2013) Genome sequence-based species delimitation with confidence intervals and improved distance functions. BMC Bioinformatics 14:60. https://doi.org/10.1186/1471-2105-14-60
18. Lee I, Ouk Kim Y, Park SC, Chun J (2016) OrthoANI: an improved algorithm and software for calculating average

nucleotide identity. Int J Syst Evol Microbiol 66(2):1100–1103. https://doi.org/10.1099/ijsem.0.000760
19. Yoon SH, Ha SM, Lim J, Kwon S, Chun J (2017) A large-scale evaluation of algorithms to calculate average nucleotide identity. Anton Leeuw 110(10):1281–2128. https://doi.org/10.1007/s10482-017-0844-4
20. Seemann T (2014) Prokka: rapid prokaryotic genome annotation. Bioinformatics 30:2068–2069. https://doi.org/10.1093/bioinformatics/btu153
21. Price MN, Dehal PS, Arkin AP (2010) FastTree 2–approximately maximum-likelihood trees for large alignments. PLoS ONE 5:e9490. https://doi.org/10.1371/journal.pone.0009490
22. Arkin AP, Cottingham RW, Henry CS et al (2018) KBase: the United States department of energy systems biology knowledgebase. Nat Biotechnol 36:566–569. https://doi.org/10.1038/nbt.4163
23. Li L, Stoeckert CJ, Roos DS (2003) OrthoMCL: identifcation of ortholog groups for eukaryotic genomes. Genome Res 13:2178–2189. https://doi.org/10.1101/gr.1224503
24. Tindall BJ (1990) A comparative study of the lipid composition of *Halobacterium saccharovorum* from various sources. Syst Appl Microbiol 13:128–130. https://doi.org/10.1016/S0723-2020(11)80158-X
25. Tindall BJ (1990) Lipid composition of *Halobacterium lacusprofundi*. FEMS Microbiol Lett 66:199–202. https://doi.org/10.1016/0378-1097(90)90282-U
26. Tindall BJ, Sikorski J, Smibert RM, Krieg NR (2007) Phenotypic characterization and the principles of comparative systematics. In: Reddy CA, Beveridge TJ, Breznak JA, Marzluf G, Schmidt TM, Snyder LR (eds) Methods for general and molecular microbiology, 3rd edn. American Society for Microbiology, Washington, DC, pp 330–393. https://doi.org/10.1128/9781555817497.ch15
27. Collins MD (1985) Analysis of isoprenoid quinones. Methods Microbiol 18:329–366. https://doi.org/10.1016/S0580-9517(08)70480-X
28. Orata FD, Meier-Kolthoff JP, Sauvageau D, Stein LY (2018) Phylogenomic analysis of the gammaproteobacterial methanotrophs (order methylococcales) calls for the reclassification of members at the genus and species levels. Front Microbiol 9:3162. https://doi.org/10.3389/fmicb.2018.03162
29. Wayne LG, Brenner DJ, Colwell RR et al (1987) International Committee on Systematic Bacteriology. Report of the ad hoc committee on reconciliation of approaches to bacterial systematics. Int J Syst Bacteriol 37:463–464. https://doi.org/10.1016/s0176-6724(88)80120-2
30. Richter M, Rossello-Mora R (2009) Shifting the genomic gold standard for the prokaryotic species definition. Proc Natl Acad Sci USA 06(45):19126–19131. https://doi.org/10.1073/pnas.0906412106
31. Luo C, Rodriguez-R LM, Konstantinidis KT (2014) MyTaxa: an advanced taxonomic classifier for genomic and metagenomic sequences. Nucleic Acids Res 42(8):e73. https://doi.org/10.1093/nar/gku169
32. Parker CT, Tindall BJ, Garrity GM (2019) International code of nomenclature of prokaryotes. Int J Syst Evol Microbiol 69(1A):S1–S111. https://doi.org/10.1099/ijsem.0.000778
33. Lefort V, Desper R, Gascuel O (2015) FastME 2.0: a comprehensive, accurate, and fast distance-based phylogeny inference program. Mol Biol Evol 32:2798–2800. https://doi.org/10.1093/molbev/msv150
34. Farris JS (1972) Estimating phylogenetic trees from distance matrices. Am Nat 106(951):645–667. https://doi.org/10.1086/282802